Available online at www.sciencedirect.com

SCIENCE DIRECT®

Journal of Molecular Catalysis A: Chemical 242 (2005) 233–240

JOURNAL OF MOLECULAR CATALYSIS A: CHEMICAL

www.elsevier.com/locate/molcata

Theoretical study of the Ga/SAPO-11 catalyst Extra-framework gallium species and *n*-butane transformation

Anibal Sierraalta[a,*], Yajaira Guillen[b], Carmen M. Lopéz[b], Ramon Martinez[a], Fernando Ruette[a], Francisco Machado[b], Marcos Rosa-Brussin[b], Humberto Soscún[c]

[a] *Laboratorio de Química Computacional, Centro de Química, Instituto Venezolano de Investigaciones Científicas, Apartado 21827, Caracas 1020-A, Venezuela*
[b] *Centro de Catálisis, Petróleo y Petroquímica, Facultad de Ciencias, Universidad Central de Venezuela, Caracas, Venezuela*
[c] *Laboratorio de Química Inorgánica Teórica, Departamento de Química, Facultada de Ciencias, Universidad del Zulia, Maracaibo, Venezuela*

Received 2 June 2005; received in revised form 3 August 2005; accepted 3 August 2005
Available online 13 September 2005

Abstract

Calculations to study the interaction of Ga^+, $[GaO]^+$ and Ga_2O with a Brönsted acid site of a SAPO-11 silicoaluminophospates were carried out using the semiempirical MSINDO approach. The SAPO-11 structure was modeled by a ring of 10 tetrahedrons and 3 rings of 10 tetrahedrons system. The calculations show that the formation of $[HGaOH]^+$ and $[GaH_2]^+$ species by reduction with H_2 are thermodynamically favored. The transformation of $[HGaOH]^+$ into Ga^+ and water is highly endothermic. The Ga_2O react with the Brönsted acid site to produce anchored species, which can be reduced by molecular hydrogen to give $[Ga(GaH)(OH)]$ and $[GaOGaH_2]$. The Ga^+ and Ga_2O reactions with *n*-butane to produces butenes are all endothermic.

Keywords: MSINDO; Ga; SAPO-11; Calculations; Gallium hydrides; Ga_2O; GaH_2

1. Introduction

Silicoaluminophospates (SAPO) molecular sieves are used in the heterogeneous catalysis research for different reaction types. For example, Pt/SAPO-5, Pt/SAPO-11, Pt/SAPO-31 [1–3] and SAPO based bimetallic bifunctional catalysts such as Ni–Pt/SAPO-5 and Ni–Pt/SAPO-11 [4], has been employed in the hydroisomerization and/or hydrocracking of *n*-heptane and *n*-hexane. Pt/SAPO-31 has shown to be a very efficient catalyst with high activity for Heck reactions of aryl chlorides [5] and SAPO-5 and ceria-modified SAPO-5 exhibited high selectivity in the isopropylation of biphenyl with high conversion (89%) [6]. Different factors have been claimed to be the responsible of the catalytic activity. Parlitz et al. [7] found that the catalytic behavior of these catalysts, not only is a function of the number and acidic strength of their active sites, but also of the pores size and the location of hydroxyl groups. Meriaudeau et al. [8] accounted the differences in isomerization products in terms of diffusional restriction and steric constraints of the SAPOs.

Recently, Ga/SAPO-11 catalyst has been used in the direct transformation of *n*-butane to *iso*-butane [9]. This catalyst, prepared by incipient wetness impregnation, has shown excellent activity, selectivity, and a high activity towards the production of isobutene using *n*-butane and H_2 as the reactants and shows a better activity than the gallium substituted silicoaluminophospates (GaAPSO-11) [10]. These promising results seem to point out the potentiality of the Ga/SAPO-11 system in the direct dehydroisomerization of light paraffins. Before the Ga/SAPO-11 can be used as a catalyst, it is reduced at high temperature in presence of H_2.

---

[*] Corresponding author. Tel.: +58 212 5041774; fax: +58 212 5041350.
E-mail address: asierral@ivic.ve (A. Sierraalta).

1381-1169/$ – see front matter © 2005 Elsevier B.V. All rights reserved.
doi:10.1016/j.molcata.2005.08.011

During this process the gallium oxide, located into the internal cavities of the SAPO-11, is partially reduced forming the active sites for the catalysis. The H_2-TPR profiles show, depending on the Ga content, two peaks, one at around 673 K related to highly dispersed Ga_2O_3 and other at around 973 K, which has been assigned of cationic $[GaO]^+$ species. This cationic extra-framework gallium species has been proposed as the responsible of the catalysis [9]. Others Ga species have been proposed in the literature too. Chao et al. [11] proposed that the Ga species exist as isolated GaO_4 units and after reduction these species are transformed into some kind of gallium hydride oligomers with bridging H atom. Others authors suggest that the gallium species exit like a dihydridegallium ion [12]. Magusin and colleagues [13] by means of chemical vapour deposition technique and using trimethylgallium (TMG) and ZSM-5 zeolite showed that this procedure leads to a homogeneous distribution of the Ga species with a Ga/Al ratio close to unity, indicating that the Ga atoms replace the Brønsted sites. Moreover, the theoretical calculations reported in the Magusin work [13] showed that it is thermodynamically more favored the reaction between the TMG with Brønsted acid site of the zeolite than with the silanol groups. According to Magusin et al. [13], after oxidative and reductive treatments, the most probably species, $[GaO]^+$ react with water

$$[GaO]^+ + H_2O \rightarrow GaO(OH) + H^+$$

with a subsequent decomposition to form gallium oxide clusters

$$2GaO(OH) \rightarrow Ga_2O_3 + H_2O$$

These reactions explain the ^{71}Ga NMR signals which had been attributed to β-Ga_2O_3, where the gallium has an octahedral oxygen coordination. Signal at 140 ppm was attributed to tetrahedral coordinate Ga^{3+} species such as $Ga(OH)_2{}^+$ coordinating to the Brønsted site. Védrine and colleagues [14] using various experimental techniques showed the presence of small GaO(OH) particles in Ga/H-ZSM-2 zeolites prepared by ion-exchange. The fact that repeated H_2-reduction and O_2-oxidation cycles increase the dispersion of gallium into the zeolite was explained considering that, in presence of H_2 at 873 K, the Ga_2O_3 can be reduced to Ga_2O that has a high vapour pressure. Therefore this species migrates into the zeolite channels and can be anchored to the zeolite. A subsequent treatment with O_2 produces GaO^+, Ga^+ or $Ga(OH)_2{}^+$ species in the ion-exchange positions.

On the other hand, Hensen et al. [15] have shown that the species of gallium in Ga/ZSM-5 can adsorb molecular hydrogen at 773 K. Analyzing the DRIFTS spectras they concluded that the following species Ga^+, $HGaOH^+$, and $(GaH_2)^+$ can be presents. The gallium hydride species are quite stable and their formation processes, by adsorption of hydrogen, is reversible at 773 K. Todorova and Su [16] by means of FTIR spectroscopy and analyzing H-ZSM-5, Ga-ZSM-5, GaPt-ZSM-5 found an IR band at 3699 cm^{-1} which was attributed to OH groups attached to Ga species as $Ga_2(OH)_xO_{3-x}$. The types of hydroxyl groups in the Ga-ZSM-5, GaPt-ZSM-5 catalysts are very sensitive to the pre-treatment.

In spite of all experimental works done, the manner in which Ga^+, $[GaO]^+$ or Ga_2O species bind to the surface of the SAPOs or are reduced by H_2 are not totally known. As a consequence, it is not clear which could be the active site of these catalysts or its structure. Therefore, theoretical studies of the interaction of these species with the Silicoaluminophospates molecular sieves are of particular interest for the understanding the reactivity and the chemistry of these systems and, the nature of the active sites of these catalysts. The present work was undertaken in order to understand the chemistry, the structure and the energy changes associated with the interaction of some Ga species with SAPO-11s. It presents the analysis of the geometries, charges and energies interaction of Ga^+, Ga_2O and GaO^+, with different T-ring models and with one H_2 molecule, using semiempirical self-consistent-field (SCF) calculations. To the best of our knowledge no theoretical studies have been done in this field and only few theoretical works on Ga-exchange ZSM-5 system have been published [17–21].

2. Computational details and molecular models

All calculations and geometry optimizations were performed using the MSINDO program [22–25] at UHF-SCF level. In order to simulate the structure of SAPO-11, two molecular models were employed. The incorporation of the Si atoms into the models was done by means of the well-known SM2 + SM3 [26,27] mechanism which avoids the formation of unstable bridges Si–O–P. The first model (S model), corresponds to a ring composed by 10 tetrahedrons (T10-ring) with 3 Si-atom, as shown in Fig. 1. The second model (L model), was constructed with three T10-rings as shown in Fig. 2. In this case, the SM2 + SM3 mechanism produces one Si island [27,28] composed by four Si atoms. Since the T10-rings are not symmetric, the position of the Si island in the S as well in the L model was varied along the structure to obtain the most stable positions. These are the structures shown in Figs. 1 and 2.

3. Results and discussion

3.1. Small model

To determine the position of the Brönsted acid site into the T10-ring, the H^+ was placed close to one oxygen atom of the ring and then, the whole structure was optimized. The results of this procedure show that the lower energy structure corresponds to the H^+ attached to the O1 atom (see Table 1 and Fig. 1), i.e., the H^+ bonded to the bridged O atom between Si and Al, followed by that at the O2 atom. The lower energy position of the H^+ into the T10-ring cannot be explained by electrostatic effects since the charges values show that the O1

Table 1
Relative energies, charges, distances and angle values for the T10 only, GaO^+/T10 and Ga/T10 systems

T10 only system: H^+ position	Relative energy (kcal/mol)	O charge before protonation	Angle
O1	0.000	−0.84	Si–O1–Al: 135.7
O2	32.6	−0.86	Al–O2–P: 145.5
O3	43.1	−0.86	Al–O3–P: 145.5
O4	51.1	−0.87	Al–O4–P: 157.7
O5	24.8	−0.87	Si–O5–Si: 157.2

GaO^+/T10 system: GaO^+ position	Relative energy (kcal/mol)	[GaO] charge O/Ga	Geometry[a] O*x*–$[GaO]^+$–O*y*
O1–O2	0.000	−0.65/+0.99	O1–Ga–O2: 80.2; Ga–O1,2: 1.84–1.93; Ga–O: 1.60
O1–O5	+4.8	−0.63/+1.00	O1–Ga–O5: 75.3; Ga–O1,5: 1.86–1.97; Ga–O: 1.60
O2–O3	+39.5	−0.58/+0.99	O2–Ga–O3: 71.0; Ga–O2,3: 1.90–1.96; Ga–O: 1.60
O3–O4	+42.0	−0.62/+1.00	O3–Ga–O4: 80.7; Ga–O3,4: 1.89–1.93; Ga–O: 1.60
O4–O6	+57.2	−0.59/+1.00	O5–Ga–O6: 69.0; Ga–O5,6: 1.97–1.97; Ga–O: 1.61

Ga/T10 system: Ga position	Relative energy (kcal/mol)	Ga charge	Geometry[a] O*x*–Ga–O*y*
O1–O2	0.000	+0.49	O1–Ga–O2: 73.9; Ga–O1,2: 1.98–2.13
O1–O5	+1.0	+0.50	O1–GaO5: 70.5; Ga–O1,5: 2.00–2.17
O2–O3	+24.0	+0.55	O2–Ga–O3: 66,6; Ga–O2,3: 2.07–2.17
O3–O4	+31.5	+0.55	O3–Ga–O4: 74.2; Ga–O3,4: 2.07–2.14

[a] Angles in °. Distances in Å. See Fig. 3.

is not the most negative oxygen atom (see Table 1). Therefore, the charge on the oxygen is not the principal factor that controls the location of the Brönsted acid site into the SAPO T10-ring. In order that the H^+ binds to an atom, it is necessary not only that the atom has a negative effective charge but the valence electrons must be in an energy level that could be accessible to the H^+ i.e.; the valence electrons must have a low ionization potential. The electrons with lower energy ionization potential are the electrons localized in the highest occupied molecular orbitals HOMOs. Therefore, it is expected that the location of the H^+ into the T10-ring correlate with the highest HOMOs that have a strong participation of oxygen atoms. The molecular orbital analysis of the T10-ring show that the HOMO orbital is mainly localized on the O1 atom which confirm the hypothesis that the position of the H^+ into the T10-ring is determined by the accessibility of the valence electron of the oxygen atom.

Cationic exchange process between H^+ and Ga^+ was modeled substituting the H^+ by the GaO^+ species in the T10-ring, as shown in Fig. 3. Table 1 shows that the optimal position for the GaO^+ species, corresponds to the bridge position

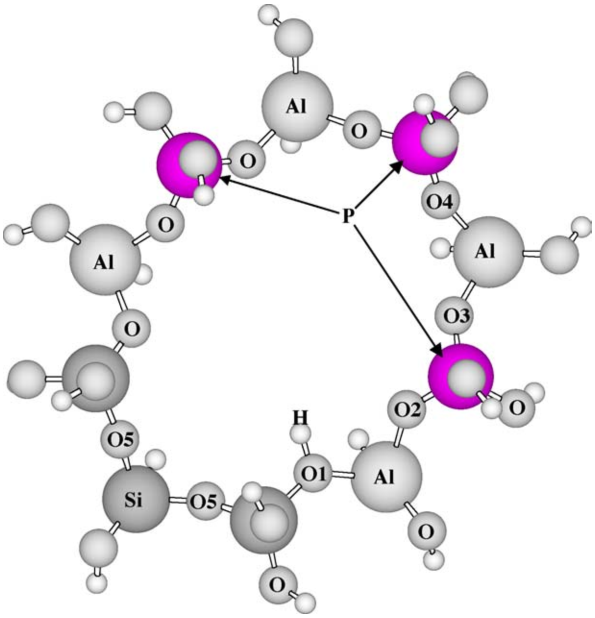

Fig. 1. Small model showing the position of the Brønsted acid site. P atoms, dark spheres. Si atoms, dark grey spheres. Al atoms, light grey spheres.

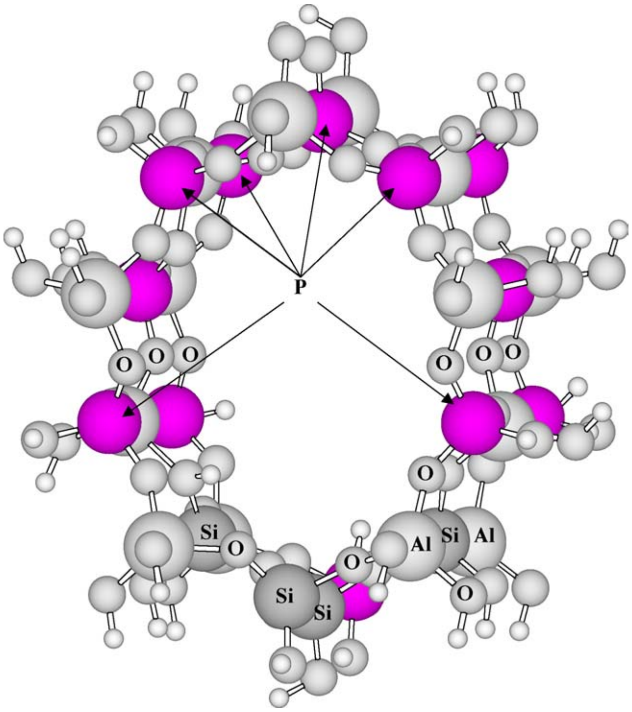

Fig. 2. Three rings model. Showing the position of the atoms. P atoms, dark spheres. Si atoms, dark grey spheres. Al atoms, light grey spheres.

between O1 and O2 atoms. The second most stable position is between O1 and O5 atoms. These results are in agreement with previous DFT calculations on the Ga-exchanged ZSM-5 catalyst [17,18,29]; where molecular dynamic results [18], as well as DFT calculations on cluster models [17,18,29], showed that the GaO^+ doubly coordinated in a bridge site is the most stable structure. The fact that the GaO^+ specie does not coordinate directly over an oxygen atom (on top) can be explained considering that the natural coordinations of Ga are the trahedrical and octahedrical. The Ga atom has the tendency to complete its coordination number of 4. This coordination is partially satisfied in the bridge position. The calculated Ga–Ox distances ($x = 1, 2, 3, 4, 5, 6$) are in the range of the experimental distances, 1.83–2.00 Å of gallium oxide Ga_2O_3. This fact, is an indication that the $[GaO]^+$ moiety can be considered as an oxidic species.

Experimentally, once the Ga is supported on SAPO-11, it is reduced by passing an H_2-flow at 773 K for 1 h [9]. To simulate computationally the reduction process, quantum calculations were performed for the positions: O1–O2, O1–O5, O2–O3, and O3–O4, considering the reaction:

$$\text{SAPO–GaO} + H_2 \rightarrow \text{SAPO–Ga} + H_2O \quad (1)$$

For all positions of the $[GaO]^+$ moiety (see Table 1), the reaction (1) is energetically favorable. Considering that, in general, the difference between the reaction energy and the reaction enthalpy less or equal to 5 kcal/mol, we can conclude from Table 2 that the reaction (1) is exothermic ($\Delta H < 0$).

According to the results reported in Table 2, for the position O1–O2 of the $[GaO]^+$, the energy change for the reaction (1) is lower than the corresponding to the positions O2–O3 and O3–O4. Therefore, it is easier to reduce the $[GaO]^+$ species when they are bonded to a Brønsted site (O1 atom) than when they are bonded to others oxygen atoms types.

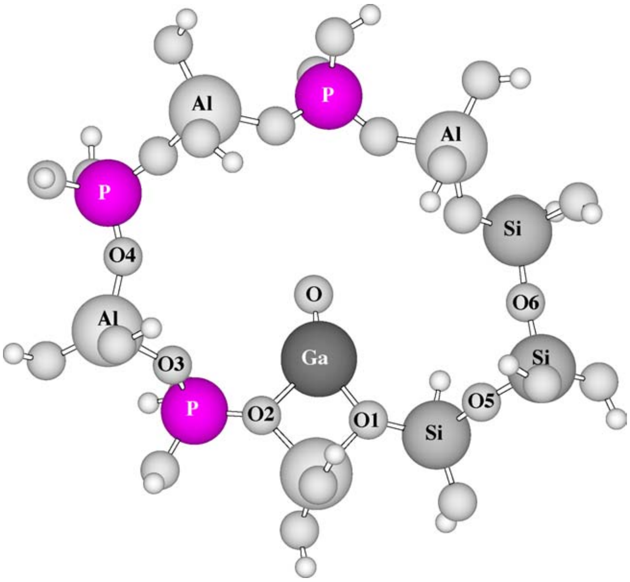

Fig. 3. T10-ring system showing the optimal position for the GaO^+. P atoms, dark spheres. Si atoms, dark grey spheres. Al atoms, light grey sphere.

Table 2
Energy changes for reduction of SAPO–GaO (reaction (1))

$[GaO^+]$ initial position	ΔE_{reac} (kcal/mol)
O1–O2	−68.5
O1–O5	−74.6
O2–O3	−83.7
O3–O4	−79.0

As expected, the charge values (see Table 1) shows that the Ga is more reduced in the SAPO–Ga than in the SAPO–GaO. Beside reaction (1), others reactions with hydrogen can occurs producing gallium hydride species:

$$\text{SAPO–GaO} + H_2 \rightarrow \text{SAPO–HGaOH}, \quad \Delta E = -111.9\,\text{kcal/mol} \quad (2)$$

$$\text{SAPO–GaO} + 2H_2 \rightarrow \text{SAPO–GaH}_2 + H_2O, \quad \Delta E = -88.4\,\text{kcal/mol} \quad (3)$$

$$\text{SAPO–Ga} + H_2 \rightarrow \text{SAPO–GaH}_2, \quad \Delta E = -20.0\,\text{kcal/mol} \quad (4)$$

Being these reactions all exothermics. According to these theoretical results, the formation of gallium dihydride species, reaction (3), as well as the formation of GaOH species (reaction (2)), could be all thermodynamically possible provided that, the entropy change be positive. This conclusion is aligned with the Bell et al. [21] results, which show that the ΔG change for reactions (1)–(3) in the Ga/H-ZSM-5 system are: −27.6, −28.6 and −13.5 kcal/mol, respectively. For the reaction (4) ΔG is positive even though the ΔH is negative [21], due to a strong entropy reduction. This phenomenon could occur in the Ga/SAPO-11 system and therefore, reaction (4) could not be thermodynamically favorable. The theoretical values calculated herein are in good agreement with the DRIFTS results, that indicate that the hydrogen adsorption by the reduced Ga species in Ga/ZSM-5 results in the formation of dihydride species [15], (see ΔE values of reactions (3) and (4)). Similarly, the formation of GaOH species has been proposed to explain the IR band at 3699 cm^{-1} that has been observed in Ga-modified HZSM-5 zeolites [16,30].

The reaction (3) can be decomposed into two steps. The first one corresponds to reaction (2) i.e., formation of the SAPO–HGaOH species. The second step, the hydrogenation of the SAPO–HGaOH species:

$$\text{SAPO–HGaOH} + H_2 \rightarrow \text{SAPO–GaH}_2 + H_2O, \quad \Delta E = +23.5\,\text{kcal/mol} \quad (5)$$

This last step is endothermic and therefore less favored, as well as the decomposition of SAPO–HGaOH species into SAPO–Ga

$$\text{SAPO–HGaOH} \rightarrow \text{SAPO–Ga} + H_2O, \quad \Delta E = +43.4\,\text{kcal/mol} \quad (6)$$

Reaction (6) presents a positive energy change greater than the corresponding to reaction (5). This energy order has been reported too for the Ga/ZSM-5 system [21]. Consequently, this suggests that reaction (6) is less favorable than reaction (5) independently of the support.

Summarizing, the most important features are as follows:

(a) The reduction processes of the SAPO–GaO species (reaction (1)) as well as the formation of Ga hydrides (reactions (3) and (4)) and oxyhydrides (reaction (2)) are all exothermic processes and thermodynamically favored provided that the entropic factor be positive.

(b) The transformation reactions of SAPO–HGaOH species into SAPO–Ga or SAPO–GaH_2 (reactions (5) and (6)) are endothermic and therefore are thermodynamically less favored than reactions (1)–(4).

3.2. *Interaction with n-butane*

As mentioned in the introduction, some authors have proposed that the transformation of *n*-butane to *iso*-butane in the Ga/SAPO-11 system is via a direct interaction with cationic extra-framework gallium species and not with hydrides or oxyhydrides species [9]. In order to analyze this proposal, quantum-chemical calculations were performed for the *n*-butane + SAPO–Ga (T10-ring) system. The calculations show that the following reactions:

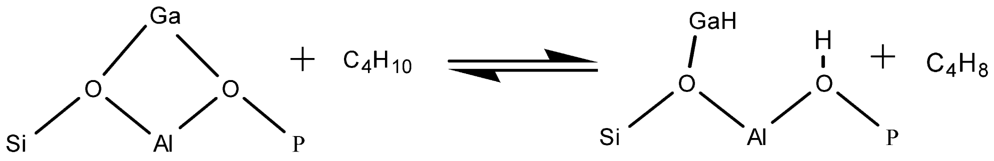

$\Delta E = 73.4$ kcal/mol ($2,3\text{-}C_4H_8$)

$\Delta E = 78.1$ kcal/mol ($1,2\text{-}C_4H_8$)

(7)

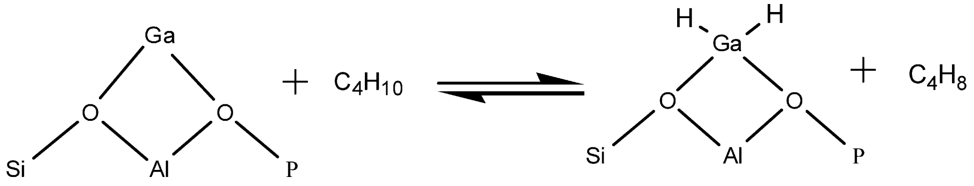

$\Delta E = 13.3$ kcal/mol $2,3\text{-}C_4H_8$

$\Delta E = 18.0$ kcal/mol $1,2\text{-}C_4H_8$

(8)

are endothermics. These results are in agreement with previous theoretical works on the dehydrogenation of ethane by $[GaO]^+$ [20] and $[GaH_2]^+$ [19,20] on zeolites. Reaction (7) is highly endothermic and therefore is less favored than reaction (8). The difference between energy values of 1,2- and 2,3-butene is due to the difference in the thermodynamic stability of 4.7 kcal/mol between both isomers. The fact that the reaction (7) be highly endothermic supports the idea that, probably, the mechanism of dehydrogenation of *n*-butane goes by a different mechanism to the classical "dehydrogenation–hydrogenation mechanism" in which the dissociative chemisorption of hydrogen atoms on the metal surface occurs [9]. This mechanism is shown in Fig. 4.

3.3. *Three ring system*

The large model or the L model was constructed with three T10-rings, one Si island located between two rings composed by four Si atoms, and two H^+. This model has two Brönsted sites with 10 probable positions for the two acidic protons H^+. These 10 structures, differentiates by the position of the H^+ into the rings. According to the calculations, the difference between the lowest and the highest energy structure is around 80.1 kcal/mol. Fig. 2 displays the lower energy structure. This structure has one H^+ in the central ring located on the bridged O between one Si and one Al, and the second H^+ in a bridge O located in one of the external ring.

It is known that the formation of Ga_2O species occurs during the reduction [13,15,25] and it is believed that these gaseous species are the responsible of the high mobility of the Ga into the zeolites upon reduction. These species can react with the support to produce the active sites. In order to get insights of this process, we proceed to study the interaction of one Ga_2O molecule with the three ring system or L model.

According to our calculations the Ga_2O molecule could be stabilized by the cage structure of the SAPO-11, being the reaction:

$$\text{SAPO–(2H)} + Ga_2O \rightarrow \text{SAPO–}Ga_2O + H_2,\quad \Delta E = -49.7\,\text{kcal/mol} \tag{9}$$

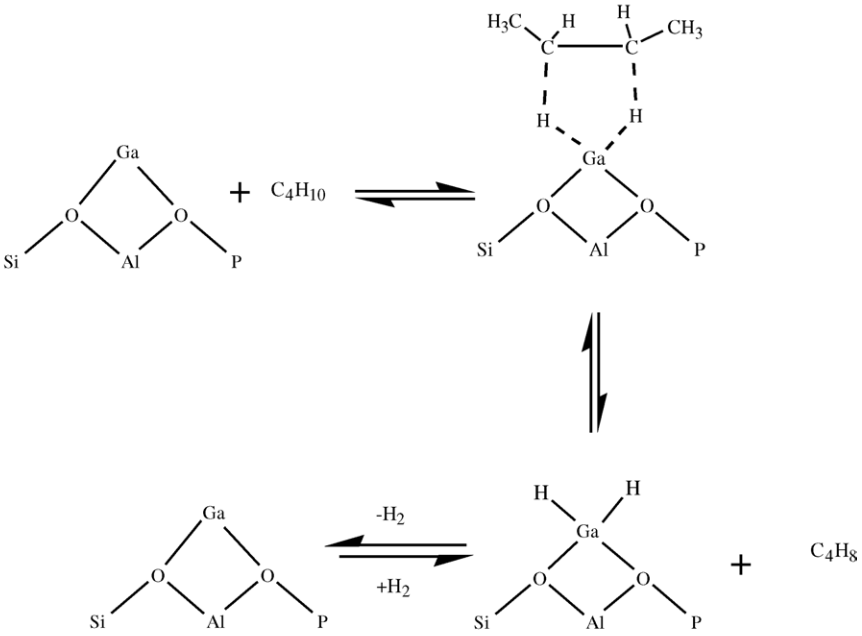

Fig. 4. Mechanism of dehydrogenation of *n*-butane with dissociative chemisorption of hydrogen atoms.

energetically favorable. The SAPO–Ga_2O minimum energy structure is displayed in Fig. 5. In this structure the Ga atoms are coordinates to the bridged O atoms replacing the H^+ atoms. One of the Ga atoms is coordinated to four framework O atoms. This high coordination produces an increase in the Ga oxidation state. As a consequence, the pentacoordinate Ga atom (Ga1, Fig. 5) is more positive ($q = +1.63$) than the Ga2 atom ($q = +0.89$), which is only bonded to two O atoms. This is an indication that the Ga is present in two oxidation states. One less reduced than the other. According to Machado et al. [9], the active site for the transformation of *n*-butane is an extra-framework Ga^+ i.e. a reduced Ga. Therefore, the Ga1 atom could be a good candidate to active site for the *n*-butane transformation.

In order to test if the stabilized Ga oxide species could be reduced by an H_2 atmosphere, we perform calculation for with the molecular aggregate SAPO–Ga_2O (see Fig. 5) and one H_2 molecule. The results show that there are several possible structures energetically favored, where the H_2 molecule is dissociated forming Ga hydride species. The three lower energy structures are displayed in Figs. 6–8. The quantum-chemical calculations show that:

$$\text{SAPO–Ga}_2\text{O (Fig. 5)} + H_2 \rightarrow \text{SAPO–Ga(GaH)(OH) (Fig. 6)}, \quad \Delta E = -87.7\,\text{kcal/mol} \qquad (10)$$

$$\text{SAPO–Ga}_2\text{O (Fig. 5)} + H_2 \rightarrow \text{SAPO–Ga–(GaH)(OH) (Fig. 7)}, \quad \Delta E = -14.3\,\text{kcal/mol} \qquad (11)$$

$$\text{SAPO–Ga}_2\text{O (Fig. 5)} + H_2 \rightarrow \text{SAPO–GaOGaH}_2\text{ (Fig. 8)}, \quad \Delta E = -0.7\,\text{kcal/mol} \qquad (12)$$

The formation of GaH(OH) species is highly favored, −87.7 kcal/mol. This is in agreement with the result of Védrine and colleagues [14] who showed experimentally the

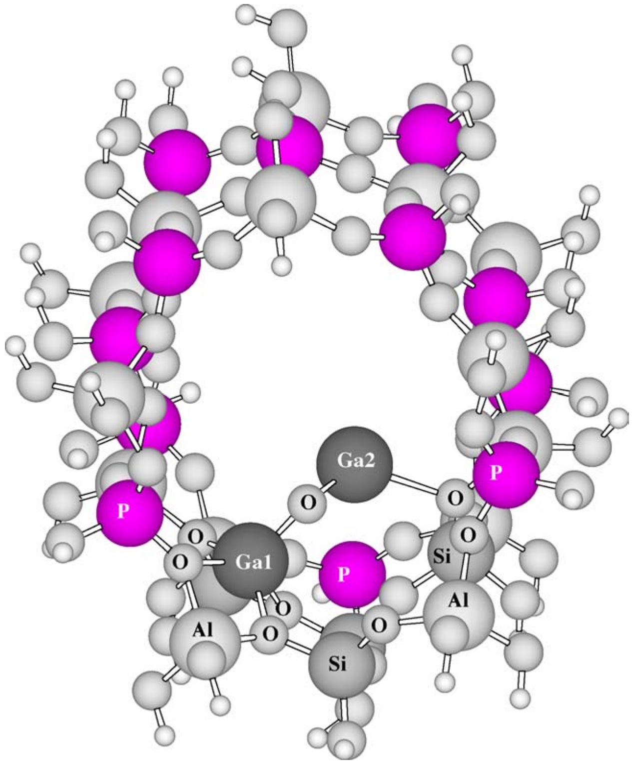

Fig. 5. Three rings system showing the minimum energy position, into a SAPO-11 structure, of the Ga_2O molecule.

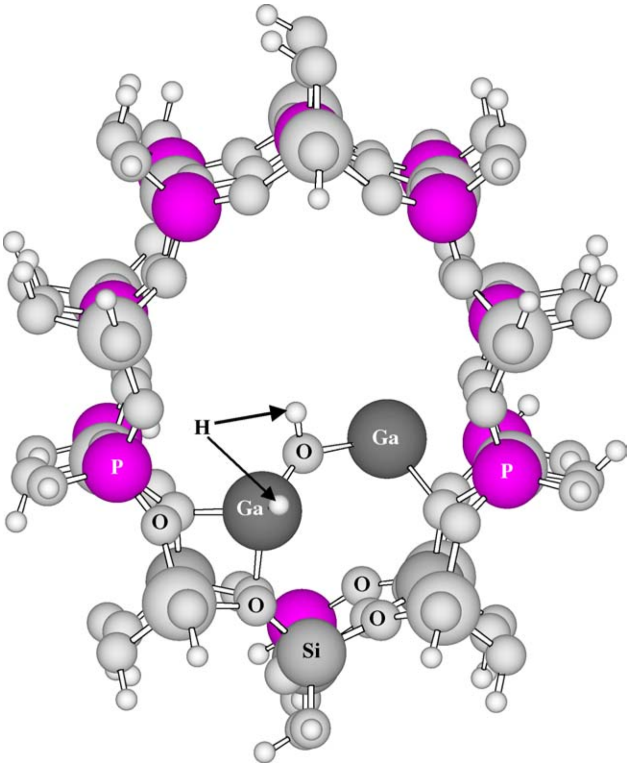

Fig. 6. SAPO–Ga(GaH)(OH) lower energy structures.

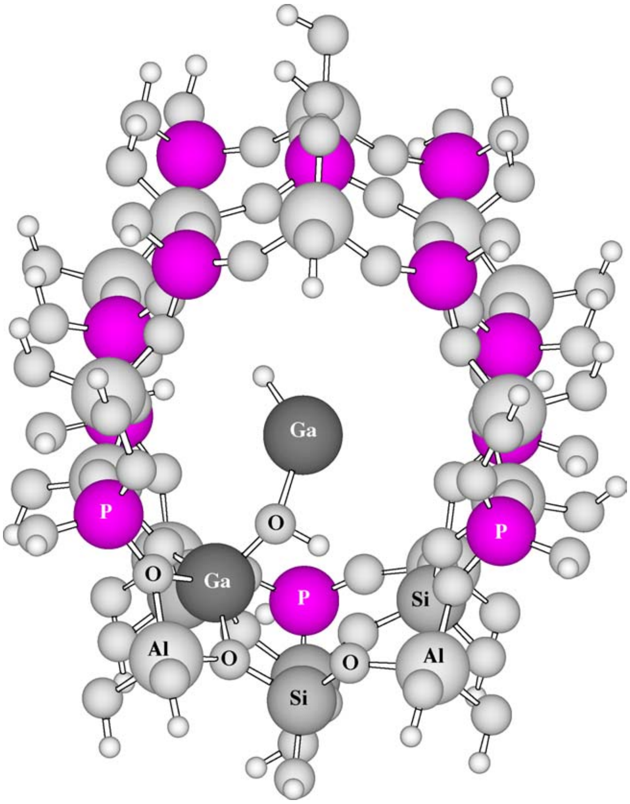

Fig. 7. SAPO–Ga–(GaH)(OH) lower energy structures.

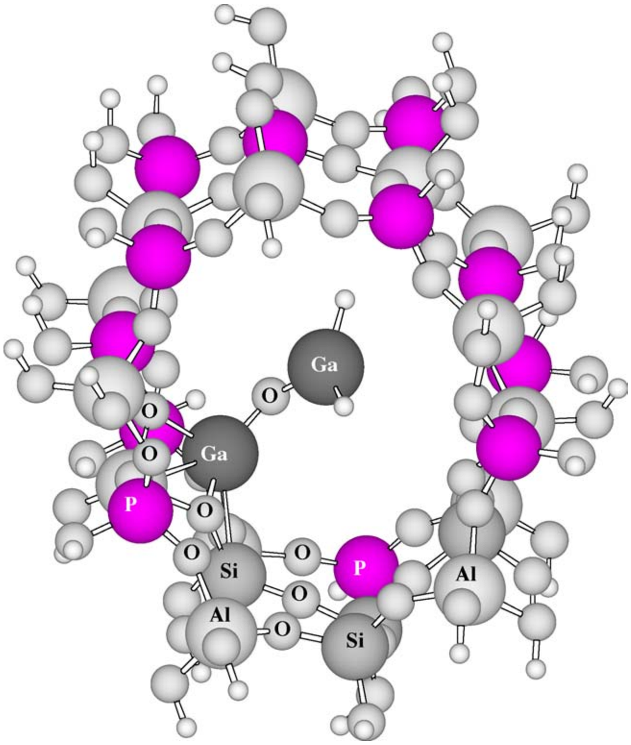

Fig. 8. SAPO–Ga(GaH)(OH) lower energy structures.

presence of OH groups bonded to the Ga atoms. In the SAPO S model, the formation of gallium dihydride is more exothermic (reaction (4)) than in the three ring system (reaction (12)), because in the three ring system the Ga atom is more bonded to and less exposed to the H_2 than in the small model. Moreover, in the three ring system, there are SAPO–Ga bonds breaking and formation of Ga–H bond. In the one ring system, there is not bond breaking and only there is a Ga–H bond formation. This indicates, that the formation of the dihydride species is more favored on Ga atom with low coordination number such as in the one ring model (see Fig. 3) than in highly coordinate Ga atoms.

Calculations for the reaction of SAPO–Ga_2O system with *n*-butane to produce butane, using the L model, show that the following reactions:

$$\text{SAPO–Ga}_2\text{O (Fig. 5)} + \text{C}_4\text{H}_{10} \rightarrow \text{SAPO–Ga(GaH)(OH)} + \text{C}_4\text{H}_8, \quad \Delta E = +35.6\,\text{kcal/mol} \tag{13}$$

$$\text{SAPO–Ga}_2\text{O (Fig. 5)} + \text{C}_4\text{H}_{10} \rightarrow \text{SAPO–Ga–(GaH)(OH)} + \text{C}_4\text{H}_8, \quad \Delta E = +23.1\,\text{kcal/mol} \tag{14}$$

$$\text{SAPO–Ga}_2\text{O (Fig. 5)} + \text{C}_4\text{H}_{10} \rightarrow \text{SAPO–GaOGaH}_2 + \text{C}_4\text{H}_8, \quad \Delta E = +122.5\,\text{kcal/mol} \tag{15}$$

are endothermics. According to the ΔE values (reactions (13)–(15)), the reaction (14) is the most thermodynamically favored, followed by reaction (13). In both reaction, occurs the formation of the (GaH)OH species

4. Conclusions

A summary of the most relevant features found in this work are: (a) The lowest energy position for Ga^+ species corresponds to a Ga^+ bonded to the oxygen atom near to the Al i.e. in the Brønsted sites. Therefore, the Ga^+ species decreases the Brønsted acidity of the SAPO-11. This is in agreement with the Brønsted acidity experimental measurement in these systems [9]. (b) Gaseous Ga_2O oxide reacts with the acidic sites of the SAPO-11 and can be anchored to the structure. This process is exothermic. (c) The anchored Ga_2O react with the hydrogen molecule to produces different structures such as [(GaH)(OH)], [GaH_2], etc. (d) The reduction of $[GaO]^+$ species into [GaH_2] is thermodynamically favored but the transformation of HGaOH into Ga^+ plus water is highly endothermic. (e) Reactions of the different Ga species studied herein with *n*-butane are endothermics. This result shows that that it is necessary high temperatures to achieve the thermodynamic spontaneity of this reaction.

Acknowledgments

The authors acknowledge the financial support given by CONIPET (Grant 97003734). We thank the support of computational framework of the FONACIT G-9700667 project.

References

[1] J.M. Campelo, F. Lafont, J.M. Marinas, J. Catal. 156 (1995) 11.
[2] J.M. Campelo, F. Lafont, J.M. Marinas, Appl. Catal. A: Gen. 152 (1997) 53.
[3] A.K. Sinha, S. Sivasanker, Catal. Today 49 (1999) 293.
[4] I. Eswaramoorthi, N. Lingappan, Appl. Catal. A: Gen. 245 (2003) 119.
[5] R. Srivastava, N. Venkatathri, D. Srinivas, P. Ratnasamy, Tetrahedron Lett. 44 (2003) 3649.
[6] M. Bandyopadhyay, R. Bandyopadhyay, S. Tawada, Y. Kubota, Y. Sugi, Appl. Catal. A: Gen. 225 (2002) 51.
[7] B. Parlitz, E. Schrier, H. Zubowa, R. Eckelt, C. Lieschke, G. Lieschke, R. Fricke, J. Catal. 155 (1995) 1.
[8] P. Meriaudeau, V.A. Tuan, V.T. Nghiem, S.Y. Lai, L.N. Hung, C. Naccache, J. Catal. 169 (1997) 55.
[9] F. Machado, C.M. Lopez, Y. Campos, A. Bolívar, S. Yunes, Appl. Catal A: Gen. 226 (2002) 241.
[10] A. Vieira, M.A. Tovar, C. Pfaaf, P. Betancuort, B. Mendez, C.M. Lopèz, F.J. Machado, J. Goldwaser, M.M. Ramírez de Agudelo, Stud. Surf. Sci. 130A (2000) 269.
[11] K.J. Chao, A.C. Wei, H.C. Wu, J.F. Lee, Micropor. Mesopor. Mater. 35 (2002) 241.
[12] G.D. Meitzner, E. Iglesia, J.E. Baumgartner, E.S. Huang, J. Catal. 140 (1993) 209.
[13] M. García-Sanchez, P.C.M.M. Magusin, E.J.M. Hensen, P.C. Thüne, X. Rozanska, R.A. van Santen, J. Catal. 219 (2003) 352.
[14] I. Nowak, J. Quartararo, E.G. Derouane, J.C. Védrine, Appl. Catal. A: Gen. 251 (2003) 107.
[15] V.B. Kazansky, I.R. Subbotina, R.A. van Santen, E.J.M. Hensen, J. Catal. 227 (2004) 263.
[16] S. Todorova, B.-L. Su, J. Mol. Catal. A: Chem. 201 (2003) 223.
[17] E. Broclawik, H. Himen, M. Yamadaya, M. Kubo, A. Piyamota, R. Vetrivel, J. Chem. Phys. 103 (1995) 2101.
[18] H. Himen, M. Yamadaya, M. Kubo, R. Vetrivel, E. Broclawik, A. Miyamota, J. Phys. Chem. 99 (1995) 12461.
[19] M.S. Pereira, M.A.C. Nascimento, Chem. Phys. Lett. 406 (2005) 446.
[20] M.V. Frash, R.A. van Santen, J. Phys. Chem. A 104 (2000) 2468.
[21] N.O. Gonzales, A.K. Chakraborty, A.T. Bell, Top. Catal. 9 (1999) 207.
[22] B. Ahlswede, K. Jug, J. Comput. Chem. 20 (1999) 563.
[23] B. Ahlswede, K. Jug, J. Comput. Chem. 20 (1999) 572.
[24] K. Jug, G. Geudtner, T. Homann, J. Comput. Chem. 21 (2000) 972.
[25] T. Bredow, G. Geudtner, K. Jug, J. Comput. Chem. 22 (2001) 861.
[26] F.J. Machado, C.M. Lopez, J. Goldwasser, B. Mendez, Y. Campos, D. Escalante, M. Tovar, Zeolitas 19 (1997) 387.
[27] G. Sastre, D.W. Lewis, C.R.A. Catlow, J. Mol. Catal. A: Chem. 119 (1997) 349.
[28] H. Tian, C. Li, J. Mol. Catal. A: Chem. 149 (1999) 205.
[29] T. Kanougi, K. Furukawa, M. Yamadaya, Y. Oumi, M. Kubo, A. Stirling, A. Fahmi, A. Miyamoto, Appl. Surf. Sci. 119 (1997) 103.
[30] C. Bigey, B.-L. Su, J. Mol. Catal. A: Chem. 209 (2004) 179.